Valery Radchenko, Dmitry V. Filosofov, Jakhongir Dadakhanov, Dimitar V. Karaivanov, Atanaska Marinova, Ayagoz Baimukhanova, and Frank Roesch*

Direct flow separation strategy, to isolate no-carrier-added ^{90}Nb from irradiated Mo or Zr targets

DOI 10.1515/ract-2015-2543
Received November 3, 2015; accepted April 13, 2016; published online June 8, 2016

Abstract: ^{90}Nb has an intermediate half-life of 14.6 h, a high positron branching of 53% and optimal β^+ emission energy of only E_{mean} 0.35 MeV per decay. These favorable characteristics suggest it may be a potential candidate for application in *immuno*-PET. Our recent aim was to conduct studies on distribution coefficients for Zr^{IV} and Nb^{V} in mixtures of HCl/H_2O_2 and HCl/oxalic acid for anion exchange resin (AG 1×8) and UTEVA resin to develop a "direct flow" separation strategy for ^{90}Nb. The direct flow concept refers to a separation accomplished using a single eluent on multiple columns, effectively streamlining the separation process and increasing the time efficiency. Finally, we also demonstrated that this separation strategy is applicable to the production of the positron emitter ^{90}Nb via the irradiation of molybdenum targets and isolation of ^{90}Nb from the irradiated molybdenum target.

Keywords: Niobium-90, zirconium, molybdenum, hydrogen peroxide, oxalic acid, anion exchange, cation exchange, UTEVA.

***Corresponding author: Frank Roesch,** Institute of Nuclear Chemistry, Johannes Gutenberg-University Mainz, Fritz-Strassmann-Weg 2, D-55128 Mainz, Germany, e-mail: frank.roesch@uni-mainz.de
Valery Radchenko: Institute of Nuclear Chemistry, Johannes Gutenberg-University Mainz, Fritz-Strassmann-Weg 2, D-55128 Mainz, Germany
Dmitry V. Filosofov, Jakhongir Dadakhanov: Dzhelepov Laboratory of Nuclear Problems, Joint Institute of Nuclear Research, Joliot-Curie 6, 141980, Dubna, Moscow region, Russian Federation
Dimitar V. Karaivanov: Dzhelepov Laboratory of Nuclear Problems, Joint Institute of Nuclear Research, Joliot-Curie 6, 141980, Dubna, Moscow region, Russian Federation; and Institute for Nuclear Research and Nuclear Energy, Bulgarian Academy of Sciences, Tsarigradsko shose 72, 1784, Sofia, Bulgaria
Atanaska Marinova: Dzhelepov Laboratory of Nuclear Problems, Joint Institute of Nuclear Research, Joliot-Curie 6, 141980, Dubna, Moscow region, Russian Federation; and University of Sofia, Faculty of Chemistry and Pharmacy, Tsar Osvoboditel Blvd. 15, 1504, Sofia, Bulgaria
Ayagoz Baimukhanova: Dzhelepov Laboratory of Nuclear Problems, Joint Institute of Nuclear Research, Joliot-Curie 6, 141980, Dubna, Moscow region, Russian Federation; and Institute of Nuclear Physics of the Republic of Kazakhstan, Ibragimov St. 1, 050032, Almaty, Kazakhstan

1 Introduction

Novel tracers based on biomolecules such as antibodies, antibody fragments and peptides were developed to address specific molecular targets overexpressed in the course of tumor growth [1–4]. Labeling and clinical use of those biomolecules with positron emitting radionuclides in the last decade have contributed to the development of a tool called *immuno*-PET [5–8]. In *immuno*-PET imaging, radionuclides are selected based on correlation with the pharmacology of these targeting vectors, such as the time needed to reach a maximal tumor-to-non-tumor ratio. This time can vary from several hours up to several days. Therefore, radionuclides with appropriate half-lives should be employed. In this context, several positron emitting radionuclides are under investigation [9, 10]. For longer lasting processes of up to one week (where the targeting vectors are typically intact antibodies), radionuclides such as ^{89}Zr ($t_{1/2}$ = 78.4 h) [11–13] and ^{124}I ($t_{1/2}$ = 100.2 h) [14, 15] are already commercially available (Table 1). For pharmacological processes lasting a few days, several radionuclides are currently under investigation for example, ^{64}Cu ($t_{1/2}$ = 12.7 h) [16–18], ^{86}Y ($t_{1/2}$ = 14.7 h) [19–22], and ^{76}Br ($t_{1/2}$ = 16.0 h) [23, 24].

In our previous studies we proposed ^{90}Nb ($t_{1/2}$ = 14.6 h) with its positron branching of 53% and an optimal β^+ energy of E_{mean} 0.35 MeV per decay as a potential candidate for labeling antibody fragments as well some intact antibodies [27, 28]. When searching for the most appropriate bifunctional chelator to attach ^{90}Nb to the biomolecules [29], desferrioxamine was examined. We were able to provide proof-of-principle by labeling ^{90}Nb with the monoclonal antibody (mAb) Rituximab and

Table 1: Decay characteristic of several PET radionuclides [25, 26] relevant to *immuno*-PET imaging (with increasing half-life).

Radionuclide	Half-life h	Main production route	$E_{\beta+\text{mean}}$ per decay in MeV (β^+ yield)	Three most intensive γ-emission in keV (abundance)
^{64}Cu	12.7	^{64}Ni(p,n)^{64}Cu ^{64}Ni(d,2n)^{64}Cu	0.05 (17.8%) also β^-, $E_{\beta^-\text{mean}}$ 0.075 (38.4%)	7.46 (X-ray) (4.8%) 7.48 (X-ray) (9.6%) 1345.8 (0.48%)
^{90}Nb	14.6	^{90}Zr(p,n)^{90}Nb	0.35 (53.0%)	141.2 (66.8%) 1129.2 (92.7%) 2319.0 (82.0%)
^{86}Y	14.7	^{86}Sr(p,n)^{86}Y	0.22 (33.0%)	627.7 (32.6%) 1076.6 (82.5%) 1153.0 (30.5%)
^{76}Br	16.2	^{76}Se(p,n)^{76}Br ^{75}As(^{3}He,2n)^{76}Br	0.64 (58.2%)	559.0 (74.0%) 657.0 (15.9%) 1853.7 (14.7%)
^{89}Zr	78.4	^{89}Y(p,n)^{89}Zr ^{89}Y(d,2n)^{89}Zr	0.09 (23.0%)	909.2 (99.0%) 1713.0 (0.75%) 1744.5 (0.12%)
^{124}I	100.2	^{124}Te(p, n)^{124}I ^{124}Te(d,2n)^{124}I	0.19 (22.1%)	602.7 (62.9%) 722.8 (10.4%) 1691.0 (11.15%)

demonstrating high labeling yields as well as stability of the labeled mAb [30]. After demonstrating the potential of ^{90}Nb in a proof-of-principle study, we continued with the development of efficient separation strategies to isolate ^{90}Nb from irradiated zirconium targets, to provide adequate radionuclidic and radiochemical purity for subsequent application for *immuno*-PET [31]. There is significant amount of literature on separation methods for Zr and Nb, mainly for the purposes of separation of uranium fission products: ^{95}Zr/^{95}Nb. That means that most of the tested and developed separations were with zirconium and niobium in no-carrier-added (nca) forms. Separation strategies including precipitation [32, 33] and a broad number of liquid-liquid extraction systems [34–37] for rapid separation were published. For the separation of bulk zirconium mass from no-carrier-added niobium, ion exchange chromatography seems to be most convenient strategy, where the small mass product can retain on the column and the bulk target mass can pass through. Several groups report efficient separation of Nb from Zr by using anion exchange resin in hydrochloric and hydrofluoric acid media [38–41]. As a common practice to achieve appropriate purity for medical application, additional purification steps are required. Based on these findings, we developed a separation strategy based on a combination of anion exchange and solid phase extraction: the two step protocol, i.e. transfer of Nb^V from ion exchange columns (allowing crude separation) to final purification by solid-phase extraction (SPE) on UTEVA resin including elution with a mixture of 6 M HCl/0.3 M H_2O_2, though working very well, still asks for further improvement and simplification. Therefore, in this work we describe a "one pot" system for the direct transfer of ^{90}Nb from the anion exchange column to the SPE cartridge, which allows, by reducing of steps, saving time, and significantly simplifies automation of this separation. Additionally, we adopted this separation strategy to the separation of nca ^{90}Nb from an irradiated molybdenum target instead of zirconium. By this separation strategy, Nb^V can be isolated from elements of the III to VII groups of the periodic table which can be present in no-carrier-added condition in the irradiated target materials.

2 Materials and methods

2.1 Materials

Reagents were purchased from Sigma-Aldrich (Germany) and used without further purification unless otherwise stated. Deionized water (18 MΩ · cm) and ultrapure HCl solution were used. No further special measures were taken regarding working under strict metal-free conditions. Ion exchange chromatography resins

AG 1 × 8 (200–400 mesh) (BioRad®) and DOWEX 50 × 8 (200–400 mesh) (BioRad®) were used. For solid phase extraction UTEVA (diamyl, amylphosphonate) resin (100–150 μm) (Triskem, France) was used. Zirconium disks of 10 mm diameter and a thickness of 0.25 mm (Strem, Kehl, Germany) were used for proton irradiations, and zirconium granules 1–3 mm, 99.8% (ChemPur, Germany), were used for neutron irradiations.

Distribution coefficients as well as the production yield, radionuclidic purity, radiochemical purity and separation yield of ^{90}Nb were determined by γ-ray spectroscopy. The γ-ray spectroscopy was performed using an Ortec HPGe detector system and Canberra Genie 2000 software. The dead time of the detector was always kept below 10%. The detector was calibrated for efficiency at all positions with the certified standard solution QCY48, R6/50/38 (Amersham, UK).

2.2 Production of $^{90/92m/95}$Nb and $^{95/88}$Zr isotopes

Radionuclides for measurement of distribution coefficients

For the determination of distribution coefficients, ^{92m}Nb ($t_{1/2}$ = 10.12 d), ^{95}Nb ($t_{1/2}$ = 35.0 d) and ^{88}Zr ($t_{1/2}$ = 83.4 d) were utilized.

For the production of ^{92m}Nb and ^{95}Nb, a molybdenum foil (0.761 g, 18 × 26 mm, 0.1 mm thickness) of natural isotopic composition was irradiated for 30 min at the Phasotron facility at the Joint Institute of Nuclear Research (JINR), Dubna, Russian Federation, at 100 ± 1 MeV proton energy and 3 μA current.

^{88}Zr was extracted from a silver metal target (1.646 g) irradiated at Phasotron facilities in JINR with proton energy ~ 660 MeV and current 2 μA for 3 h.

Radionuclides for development of separation strategies

To optimize a radioniobium/zirconium separation protocol, ^{90}Nb ($t_{1/2}$ = 14.6 h) and ^{95}Nb (35.0 d) were employed. ^{95}Nb was produced via the ^{94}Zr(n, γ) → ^{95}Zr(β^-, $t_{1/2}$ = 64 d) → ^{95}Nb process starting from natural zirconium granules (1–3 mm, 99.8% ChemPur, Germany). Neutron irradiations were performed at the TRIGA reactor at the University of Mainz, Germany, and at the research reactor BERII at the Helmholtz Centre Berlin, Germany. In the latter case, 400 mg were irradiated at a neutron flux of 2×10^{14} s^{-1} cm^{-2} (BER II) for 50 d.

Table 2: Main gamma emission energies of radionuclides used in this work [13].

Radionuclide	$t_{1/2}$ (days)	Main γ emission energies (keV)	Abundance (%)
^{92m}Nb	10.2	934.4	99.2
^{90}Nb	0.61	1129.0	92.7
^{95}Zr	64.0	724.2	44.3
		756.7	54.4
^{95}Nb	35.0	765.8	99.8

^{90}Nb was produced via the ^{90}Zr(p, n)^{90}Nb reaction at the cyclotron MC32NI of the German Cancer Research Center Heidelberg. For irradiation, a stack of three discs of natural zirconium (natural abundance 51.45% ^{90}Zr) foils of 10 mm diameter and a thickness of 0.25 mm each were used. Irradiation was performed at 20 MeV proton energy and a current of 5 μA for 1 h. This initial proton energy was decreased to 17.5 MeV entering the 1st foil of Zr by using an aluminum holder cover of 0.5 mm thickness. 24 h after end of irradiation (EOB), production yields and impurities were measured.

The activities of $^{90/92m/95}$Nb and $^{95/88}$Zr were measured by γ-ray spectroscopy. Main gamma lines used for the radionuclides are listed in Table 2.

2.3 Determination of distribution coefficients

Preparation of stock solutions

^{92m}Nb and ^{95}Nb were isolated from irradiated molybdenum targets by anion exchange chromatography. In short, molybdenum targets were placed in a plastic vial and 28 M HF (3 mL) and 16 M HNO_3 (1 mL) were added. After complete target dissolution, the mixture was loaded on a column filled with 500 mg of AG 1 × 8 resin (200–400 mesh) in F^- form. The column was washed with conc. HF (20 mL) and $^{92m/95}$Nb was eluted with a mixture of 6 M HCl/0.3 M H_2O_2 (2 mL).

^{95}Zr was extracted from irradiated silver target by using cation exchange chromatography in HNO_3 media based on previously determined K_d values [42].

After separation of the radionuclides, the corresponding fractions were evaporated to dryness and dissolved in 6 M HCl (2 mL). Stock solutions were made of: 8 ± 3 kBq of ^{92m}Nb, 4 ± 1 kBq of ^{95}Nb ($t_{1/2}$ = 35.0 d) and 7 ± 2 kBq of ^{88}Zr per 10 μL of solution.

Preparation and conditioning of resins

For the determination of distributions coefficients, the anion exchange resin AG 1 × 8, 200–400 mesh, (4 g) was used. The resin was first washed with water (10 mL), and then transferred to the Cl^- form by washing with 12 M HCl (20 mL). Finally, the resin was additionally washed with water (10 mL) to remove any excess of Cl^-, and kept until dry for 48 h at room temperature.

The UTEVA resin was applied without further preconditioning.

Procedure for distribution coefficients determination

Distribution coefficients were determined by batch mode according to the following procedures:

50 mg of resins were placed in a 2 mL tube, then 1 mL of solution of appropriate concentrations of HCl/hydrogen peroxide or oxalic acid and 10 µL of the radionuclides stock solution were added. The mixture was vigorously stirred and allowed to stay for 24 h (4 h for mixtures containing hydrogen peroxide) at room temperature. Next, the mixtures were centrifuged and 900 µL of the solution were taken and measured by γ-ray spectroscopy. The activity of the resin was determined by subtraction of activity in the solution from total activity in the sample, corrected by masses and volumes. Distribution coefficients were calculated from Equation (1), where $A_{50\ \mathrm{mg(res.)}}$ is the activity in 50 mg of the resin and $A_{50\ \mu\mathrm{L(sol.)}}$ is the activity in 50 µL of solution.

$$K_D = \frac{C^{\mathrm{eq.}}_{\mathrm{phase1}}}{C^{\mathrm{eq.}}_{\mathrm{phase2}}} = \frac{A_{1\ \mathrm{g(res.)}}}{A_{1\ \mathrm{mL(sol.)}}} = \frac{A_{50\ \mathrm{mg(res.)}}}{A_{50\ \mu\mathrm{L(sol.)}}} \qquad (1)$$

Transfer of ^{90}Nb from AG 1 × 8 to UTEVA

Based on distribution coefficients determined in batch experiments, the most appropriate mixtures of HCl and oxalic acid for the direct transfer are 0.2 M, 0.3 M, 0.4 M oxalic acid, and 9.2 M, 7.5 M, 6.9 M for hydrochloric acid. These mixtures were tested for separation conditions of 300 mg AG 1 × 8 and 100 mg of UTEVA. Aliquots of dissolved Mo and Zr targets were loaded on the anion exchange column and washed with 5 mL of 28 M HF. Next, the above described mixtures were applied. Fractions (200 µL) were collected from the anion exchanger until maximal activities of ^{90}Nb were eluted. These fractions were directly transferred to the UTEVA resin.

2.4 Separation strategy

Target dissolution

Zr target: The irradiated zirconium target, typically 260 ± 3 mg was placed into a 15 mL plastic vial and water (500 µL) was added. For dissolution, 28 M hydrofluoric acid (500 µL) was added, and after full dissolution concentrated hydrofluoric acid (1 mL) was added.

Mo target: The irradiated molybdenum target, typically 760 ± 6 mg, was placed into a 50 mL plastic vial and water (1 mL) was added. For dissolution, a mixture of 28 M HF and 16 M HNO_3 was applied. First, 28 M hydrofluoric acid (1.5 mL) was added and then 16 M HNO_3 (0.5 mL) was added dropwise. After complete target dissolution, the mixture was filled up to 5 mL with 28 M HF.

Crude separation on anion exchange column

The crude separation from Zr or Mo target was applied following a published protocol [31].

2 mL of 21 M hydrofluoric acid containing the irradiated zirconium target solution were passed through the cation exchange resin (DOWEX 50 × 8, 100 mg, 200–400 mesh, 10 × 5 mm)in H^+ form for removal of colloids, undissolved target particles and possible trace contamination of 2+ and 3+ charged metal cations, such as Cu^{2+} or Fe^{3+} from the target holder. The column was additionally washed with concentrated hydrofluoric acid (1 mL). The solution (3 mL) which passed through the cation exchange resin was transferred to an anion exchange column (300 mg, 25 × 5 mm) filled with AG 1 × 8 resin (200–400 mesh) in F^- form preconditioned with 21 M (10 mL) hydrofluoric acid. Nb^V remained on this resin and the bulk amount of Zr^{IV} passed through. The column was washed with concentrated HF (4.5 mL) to elute traces of Zr^{IV}, while $^{90/95}$Nb stayed on the column. The molybdenum target behaved similar in this system and thus was processed via similar protocol.

Direct flow transfer ^{90}Nb target solution from AG 1 × 8 to UTEVA

A small plastic column was filled with UTEVA resin (150 µm, 100 mg, 10 × 5 mm). The anion exchange column was directly connected with the UTEVA cartridge and 7 mL of 0.3 M oxalic acid/7.5 M HCl were passed through both columns.

Final purification of ^{90}Nb on UTEVA resin

The UTEVA column was next washed with 5 M HCl (5 mL). Traces of $^{*}Zr^{IV}$ passed through the UTEVA, while Nb^{V} remained absorbed on the column. For the elution of $^{90/95}$Nb, 0.1 M oxalic acid was used. The column was washed with 200 µL and $^{90/95}$Nb eluted with an additional 400 µL of 0.1 M oxalic acid. Similar protocol was applied for the molybdenum target. The decontamination factor Zr/Nb and Mo/Nb was measured by ICP-MS and γ-ray.

3 Results

3.1 Production of niobium and zirconium isotopes

^{90}Nb production via ^{nat} Zr(p,n) process

The overall (p,n) irradiation yield of ^{90}Nb for 1 h and 5 µA irradiations was 720 ± 50 MBq, i.e. 145 ± 10 MBq/µAh under the given irradiation parameters. The isotopic purity of ^{90}Nb after EOB was greater than 97%. The minor isotopic impurities found were: $^{92\,m}$Nb ($t_{1/2}$ 10.2 d) = 1.64%, ^{95}Nb ($t_{1/2}$ 35.0 d) = 0.08%, ^{95m}Nb ($t_{1/2}$ 3.6 d) = 0.29% and ^{96}Nb ($t_{1/2}$ 23.35 h) = 0.88%.

^{90}Nb and ^{90}Mo production by irradiation with high energy proton Zr and Mo via ^{nat}Zr/^{nat}Mo(p,xn) reactions

Three irradiations of natural molybdenum and zirconium targets were performed i) to determine the production yield of ^{90}Mo and ^{90}Nb and ii) to monitor the simultaneous production of other radionuclides. In Table 3, all radionuclides detected in the irradiated Mo target are listed with their activities.

The production yield of ^{90}Nb at the internal beam irradiation positron of the Phasotron facility was 258 ± 40 MBq/µAh, which is almost twice as high as for the (p,n) cyclotron irradiation [30]. A second main advantage of this production route is the excellent purity of ^{90}Nb which is formed by the decay of ^{90}Mo ($t_{1/2}$ = 5.56 h). This decay also allows additional time for transportation and handling to finally obtain ^{90}Nb from the ^{90}Mo decay. The production yield for ^{90}Mo was 289 ± 45 MBq/µAh. 24 h after end of irradiation, due to the decay of ^{90}Mo, 80% of ^{90}Nb activity produced was still measured in the target (Table 4).

Table 3: Example of radionuclide content for Mo target irradiated at Phasotron facilities with 100 MeV for 30 min with 4 µA at EOB.

Radionuclide	Half-life, $t_{1/2}$, h	Activity, MBq, EOB
^{93}Tc	2.7	767
^{95m}Tc	1440	6
^{95g}Tc	20	92
^{96}Tc	103.2	41
^{90}Mo	5.7	423
^{93m}Mo	6.9	179
^{90}Nb	14.6	350
^{92}Nb	243.6	7
^{86}Zr	16.5	100
^{89}Zr	78.4	134
^{86}Y	14.6	209
^{87g}Y	80.3	45
^{87m}Y	3	449

Table 4: Content of ^{90}Nb in Mo irradiated target as function of time after EOB.

Time (days)	EOB	24 h after EOB	72 h after EOB	120 h after EOB
Activity of ^{90}Nb (MBq)	350	281	37	5

^{95}Zr/^{95}Nb

More than 1.5 GBq of ^{95}Zr was produced at the BERII reactor after 50 d of irradiation at a flux of thermal neutrons of 2×10^{14} s^{-1} cm^{-2}. The maximum daughter activity of ^{95}Nb as generated from ^{95}Zr was obtained at ~67 d after EOB.

3.2 Determination of distribution coefficients

Values of distribution coefficients provide an understanding of the behaviour of Zr^{IV} and Nb^{V} on anion exchange resin and UTEVA in HCl/H_2O_2 and HCl/oxalic acid media in static (batch) systems.

However, the determination of K_d in HCl/H_2O_2 was associated with difficulties. A significant incubation time is needed to set up equilibrium between tracers, resin and media, but this equilibrium is impossible because hydrochloric acid reacts with hydrogen peroxide and over time changes its concentration. Therefore, 4 h was found to be the optimum incubation time to establish radionuclidic equilibrium and a negligible change in the concentration of the chemicals. Measurement errors for K_d for samples without peroxide were below 10%; for K_d below 100–10% and higher than 100–3%. The sum of errors in

values for K_d below 100 is mainly defined by the determination of activity of the resin by subtraction. All others error factors: counting statistics, weighting error, measurement error and others were estimated at 3%. For samples with peroxide, errors were up to 30%.

Zr^{IV} and Nb^{V} distribution coefficients in the system AG 1 × 8 and UTEVA – HCl/H_2O_2

Distribution coefficients for Nb^{V} in various hydrochloric acid concentrations and mixtures of HCl and hydrogen peroxide are shown in Table 5. Errors on K_d values in presence of H_2O_2 were up to 30%. To allow effective transfer of the radio-Nb fraction from the anion exchanger AG 1 × 8 to the UTEVA resin, the following conditions should be determined:

- distribution coefficients for AG 1 × 8 should be as low as possible (≤ 10), to allow easy elution of Nb fraction
- distribution coefficients for UTEVA should be as high as possible (≥ 1000), to allow sorption of Nb fraction

Table 5 shows that just several mixtures of HCl/H_2O_2 satisfy the above described conditions.

The most appropriate mixture is 9 M HCl/0.3 M H_2O_2. For anion exchange, the K_d value for Nb is 13 and for UTEVA it is 4700. Other options are 9 M HCl/0.2 M H_2O_2 and 9 M HCl/0.4 M H_2O_2 with K_d values for AG 1 × 8 vs. UTEVA resins being 16 vs. 500 and 9 vs. 730, respectively. However, these K_d values for the UTEVA resin are relatively low, and may result in some Nb breakthrough in the case of a dynamic column separation.

In Table 6, K_d values for Zr^{IV} in HCl/H_2O_2 are presented for the AG 1 × 8 and UTEVA resins. At 9 M HCl/0.3 M H_2O_2, the distribution coefficient for AG 1 × 8 is 22 and for UTEVA it is 1700, – that is, very similar to Nb.

Zr^{IV} and Nb^{V} distribution coefficients for AG 1 × 8 and UTEVA – HCl/oxalic acid

Oxalate complexes allow the elution of Nb^{V} from the anion exchange column. At the same time, the hydrochloric acid involved allows the absorbtion of radio-Nb on the UTEVA column. Table 7 lists distribution coefficients at various combinations of HCl and oxalic acid for Nb^{V}. Errors for K_d values in mixture HCl/oxalic acid were below 10%.

Due to the strategy that (1) a high concentration of oxalic acid is responsible for the elution of radio-Nb from the anion exchange column and (2) a high concentration of hydrochloric acid will absorb radio-Nb on the UTEVA

Table 5: Distribution coefficients for Nb^{V} in mixtures of HCl/H_2O_2 for AG 1 × 8 and UTEVA.

K_d ^{95}Nb	$[H_2O_2]$, M					
AG 1 × 8/UTEVA	0.0	0.07	0.15	0.2	0.3	0.4
11 M HCl		–	750/470	110/760	260/2100	250/730
10 M HCl		630/140	510/1800	505/1400	36/1400	93/1200
9 M HCl		–	703/4100	16/510	13/4800	9/730
8 M HCl		13/89	5/180	5/42	1/47	4/46
7 M HCl		8/16	3/17	3/12	2/8	
6 M HCl		5/6	5/5	3/4	4/4	
5 M HCl		3/1				

Table 6: Distribution coefficients for Zr^{IV} in mixtures of HCl/H_2O_2 for AG 1 × 8 and UTEVA.

K_d ^{95}Zr	$[H_2O_2]$, M					
AG 1 × 8/UTEVA	0	0.07	0.15	0.2	0.3	0.4
11 M HCl		–	1400/900	200/650	150/1500	200/610
10 M HCl		150/140	110/1900	94/1100	36/280	45/1600
9 M HCl		–	29/1700	28/1000	22/280	21/1600
8 M HCl		12/340	11/630	10/350	10/660	21/780
7 M HCl		8/160	11/110	17/290	18/300	
6 M HCl		8/39	14/7	15/75	19/77	
5 M HCl		9/22				

Table 7: Distribution coefficients for Nb^{V} in mixtures of HCl/oxalic acid for AG 1 × 8 and UTEVA.

K_d *Nb	oxalic acid, M								
AG 1 × 8/UTEVA	**0.005**	**0.01**	**0.02**	**0.05**	**0.10**	**0.20**	**0.30**	**0.40**	**0.45**
10.29 HCl	51	39	35	31	31				
	> 10 000	> 10 000	8065	> 10 000	> 10 000	> 10 000			
9.145 HCl	850	820	720	360	110	13			
	5800	9200	4600	6500	3100	3300			
7.995 HCl	420	190	93	10	7	5	12		
	5900	4800	2700	2000	610	160	1900		
6.845 HCl	32	10	5	3	5	5	2	2	
	1600	620	240	29	180	94	57	90	
6.28 HCl	11 ± 1	4	4	4	6	4	2	4	4
	747 ± 10	145	156	200	116	64	42	55	48

Table 8: Distribution coefficients for Zr^{IV} in mixtures of HCl/oxalic acid for AG 1 × 8 and UTEVA.

K_d *Zr	oxalic acid								
AG 1 × 8/UTEVA	**0.005**	**0.01**	**0.02**	**0.05**	**0.1**	**0.2**	**0.3**	**0.4**	**0.45**
10.29 HCl	1100	530	610	160	79				
	> 10 000	> 10 000	> 10 000	> 10 000	> 10 000				
9.145 HCl	17	12	2400	< 1	< 1	< 1			
	> 10 000	> 10 000	1000	7200	1900	1600			
7.995 HCl	< 1	< 1	< 1	< 1	< 1	< 1	< 1		
	2800	130	560	300	61	15	48		
6.845 HCl	< 1	< 1	< 1	< 1	< 1	< 1	< 1	< 1	
	69	24	8	< 1	2	< 1	< 1	4	
6.28 HCl	< 1	< 1	< 1	< 1	< 1	< 1	< 1	< 1	< 1
	14	3	2	< 1	< 1	< 1	< 1	< 1	2

cartridge, an appropriate combination of both components should be found. However, as the maximal soluble and time stable concentration of oxalic acid is 1 M and for HCl it is 12 M, some restrictions in sample preparation arose.

From the results presented in Table 7, several mixtures may satisfy the outlined concept. Appropriate results were obtained for several mixtures: 0.2 M oxalic acid/9.2 M HCl with K_d values for AG 1 × 8 = 13 and for UTEVA = 3300, as well as 0.3 M oxalic acid/7.5 M HCl and 0.4 M oxalic acid/6.9 M HCl Those mixtures seem to be promising for the "direct flow transfer" of radio-Nb from the anion exchanger to the UTEVA resin.

Another suitable mixture is also 0.005 M oxalic acid/6.28 M HCl with distribution coefficients for the anion exchanger of 11 and for UTEVA of 750.

Zr^{IV} distribution coefficients on anion exchange and UTEVA resins in mixtures of HCl/oxalic acid are presented in Table 8.

K_d values for Zr^{IV} are significantly lower for the anion exchanger and for UTEVA than for Nb^{V} in the above proposed mixtures. That can be an additional advantage for the direct flow separation strategy, as it provides additional decontamination from zirconium target material.

Direct transfer of Nb from anion exchanger to UTEVA resin

Mixtures of 0.2 M oxalic acid/9.2 M HCl, 0.3 M oxalic acid/7.5 M HCl and 0.4 M oxalic acid/6.9 M HCl were tested under dynamic conditions to find the most appropriate solution for the direct transfer of the Nb fraction between two columns.

For 0.4 M oxalic acid/6.9 M HCl more than 99% of the $^{90/95}$Nb fraction was eluted (in 2 mL, however, a breakthrough of $^{90/95}$Nb (more than 90%) was measured after 1 mL loading on UTEVA.

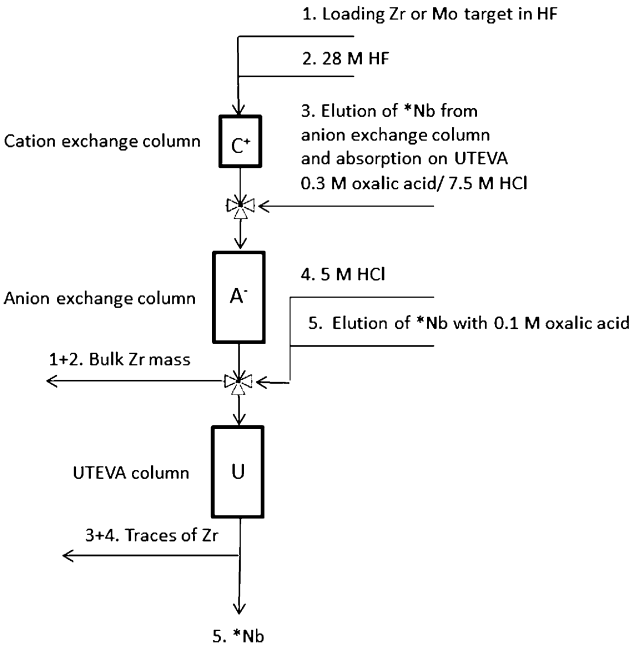

Figure 1: Direct flow separation scheme.

7 mL of 0.2 M oxalic acid/9.2 M HCl were passed through the anion exchange column, however, ≤ 10% of $^{90/95}$Nb was eluted in first two milliliters.

Finally, a 7 mL mixture of 0.3 M oxalic acid/7.5 M HCl eluted ≥ 95% of $^{95/90}$Nb from the AG 1 × 8 and the entire volume can be applied onto the UTEVA column. The same conditions can be also applied for the Mo target.

3.3 Direct flow separation strategy

The overall separation proceeds with a yield 93–95% of $^{90/95}$Nb, collected in 400 µL of 0.1 M oxalic acid. The whole separation procedure takes less than one hour, which is almost 4 times faster than the previously presented separation method [27]. The Zr/Mo decontamination factor after anion exchange was $1 \cdot 10^5$ and after UTEVA purification, $3 \cdot 10^8$. This decontamination factor equals 0.77 ng of zirconium present in the final fraction for a 260 mg zirconium target. The schematic view of the separation process is presented at Figure 1.

4 Discussions

The aim of the present work was to modify a previously developed separation strategy. The new concept was to develop a "direct flow transfer" of radio-Nb^V from an anion exchange column to a UTEVA cartridge to allow easy automation of the process and to reduce the separation time. The key was to identify combinations of hydrochloric acid and hydrogen peroxide concentrations, which will allow both the elution of radio-Nb^V from an anion exchange column and the fixation on a UTEVA cartridge. Several solution combinations seem to be appropriate, as suggested by K_d data. However, due to difficulties in the handling of peroxide solutions (building pressure, concentration instability with hydrochloric acid), that can also become a serious problem for automation, we decided to evaluate an alternative system which will allow the direct transfer of radio-Nb^V between anion exchange and UTEVA columns.

In our previous study, we used oxalic acid solution for the elution of Nb^V from a UTEVA column. We found that oxalate complexes of Nb^V can be easily eluted from a UTEVA column; however, in presence of hydrochloric acid the behaviour of complexes can change in the direction of strong sorption. Therefore, we measured K_d values of Nb^V and Zr^{IV} in mixtures of hydrochloric acid and oxalic acid to find an appropriate condition for a direct flow transfer of Nb^V. There are, finally, several concentrations where the direct transfer is possible. The next issue was the solubility of oxalic acid, for which it is difficult to prepare solutions above 1 M. Consequently, the three most suitable concentrations were tested for the online transfer. A mixture of 0.3 M oxalic acid/7.5 M HCl was found to be most suitable. 7 mL of that solution provided a transfer of 95–97% of radio-Nb^V from the anion exchange column to the UTEVA column, and no breakthrough of radio-Nb^V via the UTEVA column was measured. Another important factor is the time of the phase contact. In the case of a fast transfer velocity, some losses of $^{90/95}$Nb can be observed in terms of breakthrough on the UTEVA column. Despite using a slower velocity of the transfer, the separation time was not exceeding one hour including preparation (solutions and preconditioning columns). The overall separation yield varied between 93–95% with a decontamination factor for macroscopic Zr of ≥ 10^8.

This separation strategy was further applied to isolate nca niobium from a molybdenum target irradiated with high-energy protons. Remarkably, there is no significant difference in the behaviour of zirconium and molybdenum as the target materials, and radio-Nb is effectively separated online from macroscopic molybdenum targets in the same way as from irradiated zirconium targets. No other radionuclides were measured in final fraction of $^{90/95}$Nb.

5 Conclusions

The "direct flow" separation chemistry and technology simplifies the chemical separation of radio-Nb from irradiated Zr and Mo targets and facilitates the automation of the separation process. Separation yields vary between 93–95% with an overall decontamination factor for the macroscopic Zr or Mo targets of $\geq 10^8$. The separation time doesn't exceed 1 h, including time to precondition columns. In parallel, the developed strategy allows the separation and purification of radio-Nb^V from other co-produced nca radionuclides from the III^{st} to VI^{th} groups of the periodic table, such as Y^{III}, Zr^{IV}, Tc^{VI} and Mo^{VII}. Finally, the new separation strategy now provides a practical route to obtain the positron emitter ^{90}Nb with excellent purity and in appropriate chemical conditions for subsequent medical application.

Acknowledgement: The authors thank the teams of TRIGA reactor Mainz for the production of ^{97}Zr the research reactor BRII at Helmholtz Centrum Berlin, Germany for production of ^{95}Zr.

Many thanks to the teams of Phasotron operators at JINR for production of Nb and Zr isotopes.

Specially thanks to Dr. Steffen Happel for providing of UTEVA resin and Catherine A. L. Meyer for help in manuscript preparation.

Financial support of this project was provided by the German Science Foundation (DFG) and by the Russian Foundation for Fundamental Research grants (RFBR 15-53-12372).

Funding: Deutsche Forschungsgemeinschaft DOI:http://dx.doi.org/10.13039/501100001659 Frank Roesch.

Russian Foundation for Basic Research DOI:http://dx.doi.org/10.13039/501100002261 Dmitry V. Filosofov.

References

1. Fani, M., Maecke, H. R.: Radiopharmaceutical development of radiolabelled peptides. Eur. J. Nucl. Med. Mol. Imaging. **39(1)**, 11 (2012).
2. Rösch, F., Baum, R. P.: Generator-based PET radiopharmaceuticals for molecular imaging of tumours: on the way to THERANOSTICS. Dalton Trans. **40(23)**, 6104 (2011).
3. Zhao, H., Cui, K., Muschenborn, A., Wong, S. T.: Progress of engineered antibody-targeted molecular imaging for solid tumors (Review). Mol. Med. Rep. **1(1)**, 131 (2008).
4. Romer, T., Leonhardt, H., Rothbauer, U.: Engineering antibodies and proteins for molecular in vivo imaging. Curr. Opin. Biotechnol. **22(6)**, 882 (2011).
5. Knowles, S. M., Wu, A. M.: Advances in immuno-positron emission tomography: antibodies for molecular imaging in oncology. J. Clin. Oncol. **30(31)**, 3884 (2012).
6. van Dongen, G. A., Vosjan, M. J.: Immuno-positron emission tomography: shedding light on clinical antibody therapy. Cancer Biother. Radiopharm. **25(4)**, 375 (2010).
7. van Dongen, G. A., Poot, A. J., Vugts, D. J.: PET imaging with radiolabeled antibodies and tyrosine kinase inhibitors: immuno-PET and TKI-PET. Tumour Biol. **33(3)**, 607 (2012).
8. Pecking, A. P., Bellet, D., Alberini, J. L.: Immuno-SPET/CT and immuno-PET/CT: a step ahead to translational imaging. Clin. Exp. Metastasis. **29(7)**, 847 (2012).
9. Bhattacharyya, S., Dixit, M.: Metallic radionuclides in the development of diagnostic and therapeutic radiopharmaceuticals. Dalton Trans. **40(23)**, 6112 (2011).
10. Rice, S. L., Roney, C. A., Daumar, P., Lewis, J. S.: The next generation of positron emission tomography radiopharmaceuticals in oncology. Semin. Nucl. Med. **41(4)**, 265 (2011).
11. Vugts, D. J., van Dongen, G. A. M. S.: ^{89}Zr-labeled compounds for PET imaging guided personalized therapy. Drug Discovery Today: Technologies **8(2)**, e53 (2011).
12. Chang, A. J., De Silva, R. A., Lapi, S. E.: Development and characterization of ^{89}Zr-labeled panitumumab for immuno-positron emission tomographic imaging of the epidermal growth factor receptor. Mol. Imaging. **12(1)**, 17 (2013).
13. Chang, A. J., DeSilva, R., Jain, S., Lears, K., Rogers, B., Lapi, S.: ^{89}Zr-radiolabeled trastuzumab imaging in orthotopic and metastatic breast tumors. Pharmaceuticals **5(1)**, 79 (2012).
14. Scholten, B., Kovács, Z., Tárkányi, F., Qaim, S. M.: Excitation functions of ^{124}Te(p,xn)^{124,123}I reactions from 6 to 31 MeV with special reference to the production of ^{124}I at a small cyclotron. J. Appl. Radiat. Isot. **46(4)**, 255 (1995).
15. Koehler, L., Gagnon, K., McQuarrie, S., and Wuest, F.: Iodine-124: a promising iodine radioisotope for positron emission tomography (PET). Molecules. **15**, 2686 (2010).
16. Szelecsényi, F., Blessing, G., Qaim, S. M.: Excitation functions of proton induced nuclear reactions on enriched ^{61}Ni and ^{64}Ni: possibility of production of no-carrier-added ^{61}Cu and ^{64}Cu at a small cyclotron. J. Appl. Radiat. Isot. **44(3)**, 575 (1993).
17. Chen, K., Ma, W., Li, G., Wang, J., Yang, W., Yap, L. P., Hughes, L. D., Park, R., Conti, P. S.: Synthesis and evaluation of ^{64}Cu-labeled monomeric and dimeric NGR peptides for MicroPET imaging of CD13 receptor expression. Mo l. Pharm. **10(1)**, 417 (2013).
18. Anderson, C. J., Ferdani, R.: Copper-64 radiopharmaceuticals for PET imaging of cancer: advances in preclinical and clinical research. Cancer Biother. Radiopharm. **24(4)**, 379 (2009).
19. Roesch, F., Qaim, S. M., Stoecklin, G.: Production of the positron emitting radioisotope ^{86}Y for nuclear medical application. Int. J. Appl. Radiat. Isot. **44(4)**, 677 (1993).
20. Herzog, H., Rösch, F., Stöcklin, G., Lueders, C., Qaim, S. M., Feinendegen, L. E.: Measurement of pharmacokinetics of yttrium-86 radiopharmaceuticals with PET and radiation dose calculation of analogous yttrium-90 radiotherapeutics. J. Nucl. Med. **34**, 2222 (1993)
21. Rösch, F., Herzog, H., Plag, C., Neumaier, B., Braun, U., Müller-Gärtner, H. W., Stöcklin, G.: Radiation doses of yttrium-90 citrate and yttrium-90 EDTMP as determined via analogous yttrium-86 complexes and positron emission tomography. Eur. J. Nucl. Med. **23**, 958 (1996)

22. Nayak, T. K., Brechbiel, M. W.: ^{86}Y based PET radiopharmaceuticals: radiochemistry and biological applications. Med. Chem. **7(5)**, 380 (2011).
23. Tolmachev, V.: Bromine-labelled tracers for positron emission tomography: possibilities and pitfalls. Curr. Radiopharm. **4(2)**, 76 (2011).
24. Rossin, R., Berndorff, D., Friebe, M., Dinkelborg, L. M., Welch, M. J.: Small-animal PET of tumor angiogenesis using a ^{76}Br-labeled human recombinant antibody fragment to the ED-B domain of fibronectin. J. Nucl. Med. **48(7)**, 1172 (2007).
25. National Nuclear Data Center, Brookhaven National Laboratory, http://www.nndc.bnl.gov/.
26. Qaim, S. M., Bisinger, T., Hilgers, K., Nayak D., Coenen H. H.: Positron emission intensities in the decay of ^{64}Cu, ^{76}Br and ^{124}I. Radiochim. Acta **95(2)**, 67 (2007).
27. Busse, S., Brockmann, J., Roesch, F.: Radiochemical separation of no-carrier-added radioniobium from zirconium targets for application of ^{90}Nb-labelled compounds. Radiochim. Acta. **90**, 411 (2002).
28. Busse, S., Rösch, F., Qaim, S. M.: Cross section data for the production of the positron emitting niobium isotope ^{90}Nb *via* the ^{90}Zr(p,n)-reaction. Radiochim. Acta **90**, 1 (2002).
29. Radchenko, V., Busse, S., Roesch, F.: Desferrioxamine as an appropriate chelator for ^{90}Nb: comparison of its complexation proprieties for M-Df-Octreotide (M = Nb, Fe, Ga, Zr). J. Nuclear Med. Biol. **41(9)**, 721-7 (2014).
30. Radchenko, V., Hauser, H., Eisenhut, M., Vugts, J. D., van Dongen, G. A. M. S., Roesch, F.: ^{90}Nb – a potential PET nuclide: production and labeling of monoclonal antibodies. Radiochim. Acta **100(11)**, 857 (2012).
31. Radchenko, V., Filosofov, D. V., Bochko, O. K., Lebedev, N. A., Rakhimov, A., Hauser, H., Eisenhut, M., Aksenov, N. V., Bozhikov, G. A., Ponsard, B., Roesch, F.: Separation of ^{90}Nb from zirconium target for application in immune-PET. Radiochim. Acta **102(5)**, 433 (2014).
32. Majumdar, A. K., Mukherjee, A. K.: Separation of niobium and tantalum from zirconium with salicylhydroxamic acid. Analytica Chim. Acta **22**, 25 (1960).
33. Majumdar, A. K., Mukherjee, A. K.: Separation of niobium and tantalum with n-benzoyl-n-phenylhydroxylamine. Analytica Chim. Acta **19**, 23 (1958).
34. Yoshida, H., Yonezawa, C.: Rapid separation of niobium-95 from zirconium-95 by solvent extraction with α-benzoinoxime J. Radioanal. Chem. **5(2)**, 201 (1970).
35. Motojima, K., Hashitani, H., Bando, S., Yoshida, H.: Separation of zirconium-95, 97 and niobium-95, 97 from fission product-mixtures and irradiated uranium by an extraction method using 8-quinolinol. J. Nucl. Science Tech. **3(8)**, 326 (1966).
36. Janko, M., Herak, M. J.: Solvent extraction and separation of zirconium, niobium and tantalum by 2-carbethoxy-5-hydroxy-1-(4-tolyl)-4-pyridone. Microchim. Acta **60(2)**, 198 (1972).
37. Maiti, M., Lahiri, S.: Separation of no-carrier-added ^{90}Nb from proton induced natural zirconium target J. Radioanal. Nucl. Chem. **283(3)**, 637 (2010).
38. Steinberg, E. P.: The radiochemistry of niobium and tantalum. Subcommittee on Radiochemistry, National Academy of Sciences-National Research Council; available from the Office of Technical Services, Dept. of Commerce (1961).
39. Holloway, J. H., Nelson, F.: Ion exchange procedures: II. Separation of zirconium, neptunium and niobium. J. Chromatography A **14**, 255 (1964).
40. Dixon, E. J., Headridge, J. B.: The anion-exchange separation of titanium, zirconium, niobium, tantalum, molybdenum and tungsten, with particular reference to the analysis of alloys. Analyst **89**, 185 (1964).
41. Ferraro, T. A.: Ion-exchange separation of vanadium, zirconium, titanium, molybdenum, tungsten and niobium. Talanta **16(6)**, 669 (1969).
42. Marchol, M.: *Ion Exchangers in Analytical chemistry: Their Properties and Use in Inorganic Chemistry*. Volume 2, Prague, Czech Republic: Academia, 1982.